Fiber diameter control in electrospinning

R. Stepanyan, A. Subbotin, L. Cuperus, P. Boonen, M. Dorschu, F. Oosterlinck, and M. Bulters

Citation: Appl. Phys. Lett. **105**, 173105 (2014); doi: 10.1063/1.4900778
View online: https://doi.org/10.1063/1.4900778
View Table of Contents: http://aip.scitation.org/toc/apl/105/17
Published by the American Institute of Physics

Fiber diameter control in electrospinning

R. Stepanyan,[1,a)] A. Subbotin,[2] L. Cuperus,[1] P. Boonen,[1] M. Dorschu,[1] F. Oosterlinck,[1] and M. Bulters[1]
[1]*Materials Science Center, DSM Research, P.O. Box 18, NL-6160 MD Geleen, The Netherlands*
[2]*A. V. Topchiev Institute of Petrochemical Synthesis, Russian Academy of Sciences, Moscow 119991, Russia*

(Received 26 March 2014; accepted 17 October 2014; published online 28 October 2014)

A simple model is proposed to predict the fiber diameter in electrospinning. We show that the terminal diameter is determined by the kinetics of the jet elongation—under the influence of the electric and viscous forces—and the solvent evaporation. Numerical and simple scaling analyses are performed, predicting the fiber diameter to scale as a power 1/3 of viscosity and 2/3 of polymer solution throughput divided by electrical current. Model predictions show a good agreement to our own electrospinning experiments on polyamide-6 solutions as well as to the data available in the literature. © *2014 AIP Publishing LLC*. [http://dx.doi.org/10.1063/1.4900778]

Electrospinning is a fascinating technique to produce polymeric (nano) fibers in diameter range from tens of nanometers to several micrometers. The process itself is rather simple and versatile. A lab-spinning device generally consists of a nozzle (a needle or a protruding opening in the upper electrode) and a counter electrode, as depicted in Figure 1. A polymer solution is pumped through the nozzle and "taken up" by the applied electric field, leading to solution electrification and stretch in the air gap between the electrodes. While reaching the collector, the solution jet elongates and dries and the nanofibers (NF) are collected usually in a form of a non-woven.[1]

It is mainly the small diameter of the nanofibers and their extremely high surface to volume ratio, which makes them attractive in various application areas: air and liquid filtration, high performance textiles, wound dressing, drug delivery, tissue engineering, etc [see Huang *et al.*[2] for a more detailed overview].

For each specific application, a narrow range of NF diameters is generally required to optimize performance. Therefore, fiber diameter control is essential. However, given a lack of predictive models, the correct diameter range is often attained by trail-and-error. Although a significant amount of empirical knowledge has been accumulated over the past two decades,[3] one still lacks a comprehensive theoretical model that would allow predicting how the NF diameter depends on the solution and process parameters.

One of the first models of electrospinning[4] is based on a bead-spring simulation of a jet-flow of a charged fluid between the electrodes. Although quite comprehensive in nature, it has found a rather limited acceptance by experimentalists due to its fully numerical nature and the absence of a simple analytical relationship for the terminal fiber diameter, e.g., in a scaling form, which could be used in an everyday practice.

An alternative model[5] developed at MIT zooms into the so-called whipping part of the electrospinning jet and is built around an assumption that the terminal fiber diameter is determined by an *equlibrium* between the Coulombic repulsion between the charges on the jet's surface and the liquid's surface tension. Such an argumentation yields for the fiber diameter $d_{f,}$ up to a numerical prefactor,

$$d_f \sim \left(\gamma \frac{Q^2}{I^2}\right)^{1/3} w_p^{1/2}, \tag{1}$$

where γ is the surface tension of the polymer solution, w_p is the polymer volume fraction, Q is the flow rate, and I is the electric current in the system, so that I/Q corresponds to the electric charge per unit volume of the jet. Interestingly, experiments[5] on polycaprolactone solutions showed a perfect agreement with the predicted $(Q/I)^{2/3}$ power law. However, there is a serious deficiency in formula (1) as it states that the terminal fiber diameter is independent of liquid viscosity and evaporation conditions, in contradiction to the common experience.[6–8]

In this paper, we present a simple electro-hydrodynamic model of the jet elongation, which includes all the essential elements governing the final fiber diameter. We will show that, in contrast to the predictions of Eq. (1), it is the *kinetics* of elongation and evaporation, which governs the NF diameter, rather than the equilibrium between the Coulombic repulsion between the charges on the jet's surface and the

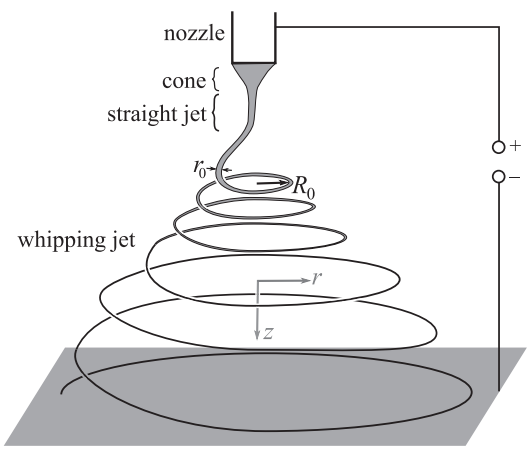

FIG. 1. Schematic representation of an electrospinning device and a polymer jet.

a)roman.stepanyan@dsm.com

liquid's surface tension. The viscosity of the polymer solution will organically enter the quantitative model and will turn out to have a profound influence on the diameter. We will also show that the predicted scaling laws are very well supported by the experiments, both our own and available in the literature.[5,6]

In general, the jet thinning process can be divided into several stages, as depicted in Figure 1. At the bottom of the nozzle, a so-called *Taylor cone* is formed: its walls carry charges brought by a conductive current from the upper electrode.[9] Further downstream, the cone goes over into a *straight charged jet*. Also, the nature of the charge transport changes from the conductive current in the cone part to a *convective* charge transport in the jet:[10] charge is virtually "frozen" onto the surface of the jet and is moved down only by advection, together with the jet. Typically, the jet diameter at the end of its straight part is insensitive to the nozzle dimensions[11] and is of the order of 10 μm for the solutions studied here.

Soon, the jet loses its stability against radial distortion[12] leading to bending and almost horizontal orientation of the fiber in the *whipping jet* zone. The jet is observed as loops of growing size, until evaporation stops their further stretch by solidification. In practice, the main thinning of the fiber occurs in the whipping zone. Stretching ratios up to several thousands are observed before solidification, giving rise to fiber diameter in submicron range. Note that, as already mentioned, jet conductivity does not play any role in charge transport anymore. Also, for the sake of simplicity, we assume the electrical discharge from the jet is negligible. Hence, the amount of charge per unit of volume of polymer stays constant at the value of $I/(Qw_{p0})$ all throughout this zone, with w_{p0} being the initial volume fraction of polymer.

Note that the jet elongation in the straight jet part is mainly due to the external electric field acting in vertical direction, Figure 1. At the same time, after the whipping instability sets in, the jet takes form of loops oriented almost completely in the horizontal plane.[1] Hence, the elongation and thinning of those loops is almost solely due to repulsion between the charges confined on the jet's surface, whereas the external electric field merely transports the loops vertically, in the direction of the collector electrode.

Such a qualitative picture inspires us to model the jet elongation and thinning in the whipping part using an analogy with dynamics of a charged liquid torus growing in the radial direction due to its own charge. We assume the initial torus dimensions are known, Figure 1, with $2r_0$ being the diameter of the jet at the beginning of the whipping zone and the initial loop radius R_0 characterized by the wavelength of the fastest growing mode of the radial instability.[12]

Further, we assume the loop radius R always exceeds the jet's one r ($R \gg r$) and express the time evolution of the torus dimensions via a balance of electric, viscous, and surface tension forces under an assumption that the inertial effects are not important. It is also assumed that no jet splitting[1] takes place.

The electrostatic contribution is obtained from the potential energy of a charged torus (here and further on, we use CGS units in all formulas) $U_E = q^2/(2\pi R)\ln(8R/r)$, where $q = V_0 I/Q$ is the torus total charge, $V_0 = 2\pi^2 R_0 r_0^2$ is the torus initial volume. Hence, the evolution equation reads

$$\pi r^2 \left(\frac{q}{V}\right)^2 \ln\frac{4V}{\pi^2 e^{3/2} r^3} - \frac{\gamma}{r} = N_1. \tag{2}$$

Here, the first term describes the electrostatic repulsion stress, with V being the volume of the torus and e denoting the natural logarithm's base. The second term is responsible for the surface tension, and N_1 is the first normal stress difference encompassing all the viscoelastic effects. Both r and V are functions of time. The time evolution of the volume $V(t)$ is controlled by the evaporation kinetics

$$\frac{dV}{dt} = -\frac{2V}{r}\Phi, \tag{3}$$

with Φ being the evaporation flux. For the sake of simplicity, we take $\Phi = k[c_s(t) - c_s^{air}]$, where c_s and c_s^{air} are the solvent concentrations in the polymer solution and in the ambient air, respectively, and k is a phenomenological constant. As for all the relevant conditions, prior to the solidification of the fiber, $c_s \gg c_s^{air}$ and $c_s = \rho_s(1 - w_p)$, we obtain

$$\Phi \simeq k\rho_s(1 - w_p), \tag{4}$$

where ρ_s is the solution density[13] and w_p is the polymer volume fraction. Finally, the polymer mass conservation dictates that $V(t)w_p(t) = V_0 w_{p0}$.

To close the set of equations (2)–(4), one needs to provide a constitutive relation which would connect the viscoelastic contribution N_1 to the elongation rate $\dot{\epsilon}$. As the rate $\dot{\epsilon}$ is determined by the time evolution of the jet (torus) radius r via[14] $\dot{\epsilon} = -2(\dot{r} + \Phi)/r$, Eqs. (2) and (3) together with (4) and the mass conservation, will provide a closed set of equations to reveal the time evolution of $r(t)$ and $w_p(t)$.

Let us first perform a qualitative analisys by assuming the solution behavior is Newtonian, i.e., $N_1 = 3\eta(w_p)\dot{\epsilon}$, where a concentration dependent shear viscosity $\eta(w_p) = (w_p/w_{p0})^{\alpha}\eta_0$ has been introduced and α is an empirical constant; η_0 denotes the initial viscosity of the solution. Before proceeding, it is convenient to rewrite Eqs. (2) and (3) in a dimensionless form. For this purpose, we introduce a new dimensionless radius variable $x = r/r^*$, where r^* is some characteristic fiber radius, whose value will be obtained later on. We also rescale the torus volume, using $\psi = V/V_0 = w_{p0}/w_p$. This leads to

$$\frac{x^2}{\psi^2}\ln\frac{4\chi\psi}{\pi^2 e^{3/2} x^3} - \frac{x_f}{x} = \frac{3}{\psi^{\alpha}} t_v \dot{\epsilon}, \tag{5}$$

$$t_{ev}\frac{d\psi}{dt} = -\frac{\psi}{x}\left(1 - \frac{w_{p0}}{\psi}\right), \tag{6}$$

where $\chi = V_0/r^{*3}$. Here, we have also introduced $t_v = \eta_0(Q/I)^2/(\pi r^{*2})$, $t_{ev} = r^*/(2k\rho_s)$, and $x_f = \gamma(Q/I)^2/(\pi r^{*3})$.

The physical meaning of the two time constants t_v and t_{ev} is clear. The first one t_v, used to non-dimensionalize the forces balance (5), is the typical time scale of elongation under the influence of electric and viscous forces—we shall call it an *electro-viscous* time. The other time t_{ev} is a characteristic time scale for the solvent evaporation and, hence, the solidification of the fiber.

It is interesting to point out that the electro-viscous time t_v increases with decreasing the characteristic fiber radius r^*, whereas evaporation time t_{ev} becomes shorter. As according to the qualitative picture outlined above, the jet thinning is determined by an interplay between the elongation and the evaporation kinetics; one can argue that the terminal fiber size corresponds to the typical radius when *the electro-viscous and the evaporation time scales become approximately the same*, i.e., at $r^* = (2k\rho_s\eta_0/\pi)^{1/3}(Q/I)^{2/3}$, when $t_v = t_{ev} = (\eta_0/\pi)^{1/3}[Q/(2k\rho_s I)]^{2/3}$.

Such a simple argument leads to a scaling formula for the fiber's terminal radius

$$r_f \sim (k\rho_s\eta_0)^{1/3}\left(\frac{Q}{I}\right)^{2/3}. \quad (7)$$

Please note that although derived by completely different arguments than used by Fridrikh *et al.*[5] to derive (1), it features the same dependency on the ratio Q/I. Additionally, it states that the final fiber diameter is dependent on the evaporation rate k and the solution viscosity η_0 with a power law exponent 1/3: both these predictions will be verified by an experiment later on.

In fact, the scaling law (1) predicted in Ref. 5 can be derived from the forces balance (5) in the limit of very slow evaporation. It corresponds to an "equlibrium" solution of (5), when elongation is stopped only when the electrostatic forces are balanced by the surface tension.

To consider viscoelastic effects and to go beyond the simple scaling predictions like (7), Eqs. (2) and (3) have to be supplemented by an appropriate constitutive relation to determine the viscoelastic contribution N_1 in the momentum balance (2). We do so by employing a Rolie-Poly modification by Kabanemi and Hétu,[16] which not only accounts for all the major relevant molecular contributions to entangled polymer solution viscoelasticity but also includes the effect of finite polymer chain extensibility and, therefore, is applicable to fast extensional flow. In our approach, all the material functions in Rolie-Poly, such as, e.g., the relaxation times, are concentration-dependent and change in the course of the jet elongation and drying according to semi-phenomenological power-laws, following from the tube theory and experiments.[17]

Typical calculation results with parameters corresponding approximately to the polyamide-6 (PA6) solutions in formic acid (FA), used in the experimental section, are shown in Figure 2. Interestingly, it turns out that our simple estimate (7) does predict the correct scaling of the diameter. In Figure 2, the calculation results for two different molar masses are shown. An important observation at this point is that when plotted as a function of the (initial) solution viscosity, the two curves are very close to each other. Hence, not the solution concentration or the polymer molar mass separately but the resulting viscosity is the key parameter determining the nanofiber dimensions. Moreover, as Figure 2 illustrates, a correlation between the fiber diameter and the viscosity is very close to *a power law with exponent of 1/3*, exactly as has been suggested by equation (7).

Such an agreement between the simple scaling estimate (7) and the numerical solution is quite intriguing. Indeed, an

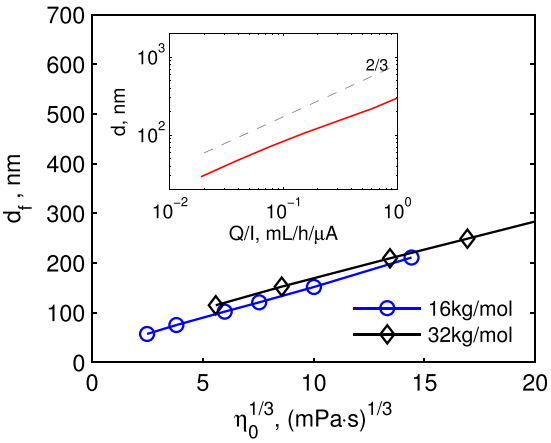

FIG. 2. Fiber end diameter as a function of viscosity, as predicted by the numerical model for PA6 solutions. Calculation is performed by varying the polymer concentration for two different molar masses. Inset: Fiber diameter shows 2/3 power law scaling with Q/I.

estimate (7) is based on an assumption that the polymeric solution can be described as a Newtonian fluid, and, hence, its elongational viscosity is simply three times its shear viscosity. In case of a viscoelastic liquid, as the one described by the Rolie-Poly constitutive law, the elongational viscosity is a nontrivial function of the elongation rate $\dot{\epsilon}$. It turns out that in the regime considered here, the viscoelastic response of the polymer is dominated by the high flow rate elongational viscosity, when the polymer chains are oriented and stretched. However, for the case of a polymer solution with a reasonably narrowly distributed molar masses, there is an almost one to one correspondence between the shear and the high flow rate viscosities: two solutions having the same shear viscosity will also have similar high flow rate extensional viscosities. This allows Eq. (7) to hold *on a scaling level*.[18,19]

Not only the scaling relation with viscosity but also the 2/3 power law dependency on the volume charge density, as expressed by the parameter Q/I, is supported by the numerical calculation (see inset in Figure 2). Finally, the scaling of fiber diameter with the evaporation speed can be demonstrated to yield a power law exponent close to 1/3 (not shown here), in accordance with (7) too.

The good correspondence between the scaling prediction and the numerical results gives one freedom of using a simple estimation for the nanofiber diameter (7).

The theoretical predictions have been tested by comparing them to our own experiments as well as to the data available in the literature. Unfortunately, in the majority of the published work, insufficient information is given on the polymer solution and the spinning process parameters. This limits our ability to perform a numerical simulation for those systems. However, certain features, such as scaling laws, can be easily verified.

Fridrikh *et al.*[5] studied electrospinning of polycaprolacton solutions: a relatively low conducting system, which allows a wide variation of flow rate and electric current. They observed a very clear $d_f \sim (Q/I)^{2/3}$ scaling by varying the flow rate to electric current ratio by about 2 orders of magnitude. Interestingly, the authors of Ref. 5 have interpreted their experimental results as a proof of their

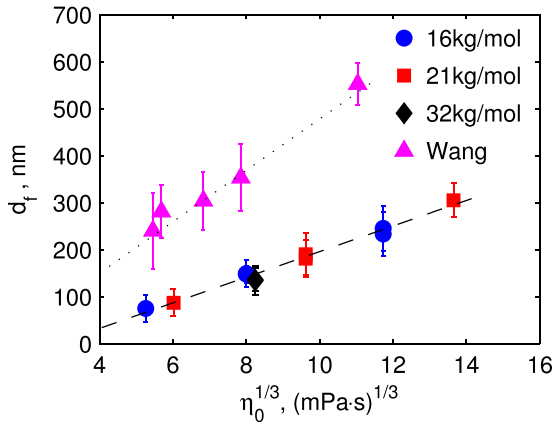

FIG. 3. Experiment: PA6 solutions (in FA) of three different molar masses $M_n = 16$, 21, and 32 kg/mol at different concentrations. Also data from Wang *et al.*[15] for PAN in DMF are shown.

theoretical model, expressed by Eq. (1), as discussed earlier. However, as we see now, completely different kinetic arguments, raised in the present work, also lead to the same scaling.

In a recent work of Cai and Gevelber,[6] the effect of evaporation rate has been carefully studied for polyvinylpyrrolidone in alcohol solutions. By introducing different alcohols as a solvent (methanol, ethanol, 1-butanol), the authors observed that the final fiber diameter scales as a power 1/3 of the evaporation rate [see Figure 19 in Ref. 6], in accordance with our prediction.

The role of viscosity has been emphasized in many works. Nevertheless, we are not aware of a systematic electrospinning study where polymer solutions of different molar masses and concentrations were compared at identical spinning conditions. Therefore, we have electrospun PA6 solutions with the number average molar mass ranging from 16 to 32 kg/mol by dissolving them in a formic acid at concentrations of 10%, 15%, and 20%. A special care has been taken to keep the spinning conditions similar.

The nanofibers so produced were investigated by scanning electron microscopy followed by image analysis, allowing to measure the final fiber diameter in a statistically sound way. The results are presented in Figure 3. Clearly, linear scaling with viscosity in power 1/3 is observed, exactly as predicted by (7). Moreover, a reasonable quantitative agreement is reached with the results of the numerical model, depicted in Figure 2.

The validity of the diameter correlation to solution viscosity is not limited to a PA6 system. For example, as also shown in Figure 3, the data of Wang *et al.* [15] on polyacrylonitrile (PAN) in dimethylformamide (DMF) solutions of varying concentration obey 1/3 power law too. The PAN/DMF system does lead to thicker diameters than PA6 solutions of comparable viscosity, mainly due to much lower conductivities of the former, resulting in higher Q/I ratio.

In summary, based on the experimental evidence, one can conclude that the model presented here adequately describes the fiber formation process during electrospinning. Our model emphasizes the kinetic nature of the mechanism controlling the final fiber diameter, with two competing processes—elongation and evaporation—responsible for the end result. The two relevant time scales corresponding to each of these processes—visco-electric t_v and evaporation t_{ev} times—are identified. Further analysis leads to a simple yet appealing relation between the fiber diameter and the material and the process parameters, Eq. (7). The predicted scaling of diameter with all the relevant quantities—viscosity, evaporation rate, and charge density—is fully supported by the experiments on different polymer solutions. Moreover, the computational model allows achieving quantitative agreement to the experimental data.

The authors thank Professor G. C. Rutledge, Professor E. J. Kramer, and Professor E. W. Meijer for useful remarks. A. Subbotin acknowledges financial support from the Russian Foundation for Basic Research (Grant No. 14-03-00299).

[1]D. H. Reneker, A. L. Yarin, E. Zussman, and H. Xu, Adv. Appl. Mech. **41**, 43 (2007).
[2]Z.-M. Huang, Y.-Z. Zhang, M. Kotaki, and S. Ramakrishna, Compos. Sci. Technol. **63**, 2223 (2003).
[3]C. Wang, Y.-W. Cheng, C.-H. Hsu, H.-S. Chien, and S.-Y. Tsou, J. Polym. Res. **18**, 111 (2011).
[4]A. L. Yarin, S. Koombhongse, and D. H. Reneker, J. Appl. Phys. **89**, 3018 (2001).
[5]S. V. Fridrikh, J. H. Yu, M. P. Brenner, and G. C. Rutledge, Phys. Rev. Lett. **90**, 144502 (2003).
[6]Y. Cai and M. Gevelber, J. Mater. Sci. **48**, 7812 (2013).
[7]S.-Y. Tsou, H.-S. Lin, and C. Wang, Polymer **52**, 3127 (2011).
[8]P. Heikkilä and A. Harlin, Eur. Polym. J. **44**, 3067 (2008).
[9]J. Fernández de la Mora, Annu. Rev. Fluid Mech. **39**, 217 (2007).
[10]J. J. Feng, Phys. Fluids **14**, 3912 (2002).
[11]A. Subbotin, R. Stepanyan, A. Chiche, J. J. M. Slot, and G. ten Brinke, Phys. Fluids **25**, 103101 (2013).
[12]Y. Shin, M. M. Hohman, M. P. Brenner, and G. C. Rutledge, Appl. Phys. Lett. **78**, 1149 (2001).
[13]We also assume that the polymer solution and the solvent have approximately the same mass density.
[14]By definition, $\dot{\epsilon} = \dot{R}/R$. As the torus volume is $V = 2\pi^2 R r^2$ and $\dot{V}$ is given by (3), one arrives at $\dot{\epsilon} = -2(\dot{r} + \Phi)/r$.
[15]C. Wang, H.-S. Chien, C.-H. Hsu, Y.-C. Wang, C.-T. Wang, and H.-A. Lu, Macromol. **40**, 7973 (2007).
[16]K. K. Kabanemi and J.-F. Hétu, J. Non-Newt. Fluid Mech. **160**, 113 (2009).
[17]M. Doi and S. Edwards, *The Theory of Polymer Dynamics* (Clarendon Press, Oxford, 1986), p. 391.
[18]Such a "correspondence" between the two viscosities breaks if one, e.g., considers blends of high and low molar masses. Then two polymer solutions of the same shear viscosity can have vastly different properties in fast elongational flow, as is the case, e.g., for a PEO/PEG system studied in Ref. 19. In fact, such blends also show a considerable departure from the master curve observed in experiment Figure 3. The results for blends are not discussed here.
[19]J. H. Yu, S. V. Fridrikh, and G. C. Rutledge, Polymer **47**, 4789 (2006).